Proceedings of IMECE2006
2006 ASME International Mechanical Engineering Congress and Exposition
November 5-10, 2006, Chicago, Illinois USA

IMECE2006-15963

Thermal Analysis for Cryosurgery of Nodular Basal Cell Carcinoma

Feng Sun[1], G. Aguilar[2], K. M. Kelly[3], G. –X. Wang[1*],

[1]Department of Mechanical Engineering, The University of Akron, OH 44325
[2]Department of Mechanical Engineering, University of California Riverside, CA 92521
[3]Beckman Laser Institute, University of California, Irvine, CA 92612

ABSTRACT

Basel cell carcinoma (BCC) is the most common human skin malignancy. Its incidence has increased significantly in Australia, Europe and North America over the past decade. A number of modalities are currently used for treatment of BCC, including cryosurgery which offers a potential for high cure rate, low cost, minimal bleeding and good cosmetic effect. However, cryosurgery is not used frequently for BCC because no current method exists to design adequate treatment parameters. We present a numerical analysis on the thermal history of the target tissue during cryosurgery of a nodular BCC using liquid nitrogen (LN_2) spray. The model uses Pennes equation to describe the heat transfer within the target tissue. A convective thermal boundary is used to describe the heat interaction between the tissue and LN_2, and the apparent heat capacity method is applied to address the tissue phase change process. A parametric study is conducted on the convective heat transfer coefficient (h_s: 10^4~10^6 W/m^2·K), cooling site area (r_s/R_0: 0.5~1.0) and spray time (t: 0~30 sec.), with the objective to understand the thermal history during tissue freezing, including lethal temperature (-50 ^{o}C) and cooling rate (CR). Results demonstrate that propagation of the lethal isotherm is sensitive to the convective heat transfer coefficient, h_s, with a range of 10^4~5×10^4 W/m^2·K. Increasing the cooling site area can significantly enhance cooling efficiency, producing dramatic increase in the amount of tissue encompassed by the lethal isotherm. The cooling rate (CR) shows a highly dynamic distribution during the cooling process: the highest CR drops quickly from 140 ^{o}C/sec. (t=0.5 sec.) to 20 ^{o}C/sec. (t=5 sec.). The highest CR is initially located close to the cooling site but moves toward the inside of the tissue as treatment proceeds.

The model presented herein provides a simulation tool for treatment planning of cryosurgery using LN_2 spray, in which the protocol parameters, e.g. cooling site area and spray time, can be determined for an optimal outcome. The quantitative predictions on the propagation of lethal isotherm and the distribution of CR should help to optimize cryosurgery efficacy.

INTRODUCTION

Basal cell carcinoma (BCC), arising from the basal layer of epidermis, is the most common human skin malignancy. BCC appears predominantly in sun-exposed areas of the skin and primarily affects the light-skinned population [1, 2]. The incidence of BCC has dramatically increased in US, Canada, Europe and Australia, over recent decades, possibly due to increased sun-exposure associated with traveling, sunbathing and other leisure activities [3]. In the United States, the annual incidence of BCC is 146 per 100,000. Australia has the highest annual incidence, 726 per 100,000 [4]. A number of therapies are available for BCC, including Mohs surgery, photodynamic therapy, topical imiquimod, radiation therapy, and cryosurgery [3]. Cryosurgery utilizes low temperatures and tissue freezing to destroy the tumor and has several merits, including a high cure rate, low cost, relative ease of implementation, minimal or no blood loss and good cosmetic outcome.

Cryosurgery has been utilized in dermatological practice since the late 19th century [5]. Liquid air was used as the first cryogen but was later replaced by solid CO_2, liquid oxygen and

* Corresponding author: gwang@uakron.edu

liquid nitrogen (LN_2). LN_2 is to date the most commonly used cryogen because of high cooling efficiency, low cost and wide availability. There are two main LN_2 treatment techniques: cryosurgical probe (cryorpobe) and cryosurgical spray (cryospray). Cryoprobe is a closed heat exchanger, cooled by the inner flow of LN_2. The continuous circulation of LN_2 within the probe relies on a complex instrument system which provides storage, super-cooling, pumping, and LN_2 delivery [6]. The cryospray technique uses a simple handheld spray device, composed of a Dewar tank, delivery pipe, trigger and changeable nozzles. Cryospray is superior to other simple delivery methods, e.g. the swab method (applying LN_2 onto target tissue by a LN_2-soaked cotton swab), which can produce a freezing depth of no more than 2 mm under the skin surface [7]. Simplicity of implementation and the strong cooling capacity associated with the cryospray technique make it a useful therapeutic modality for a variety of skin lesions including BCC [1, 3].

Studies indicate that target tissue thermal history plays a critical role in cryosurgical injury outcome. Several numerical studies have addressed cryosurgical tissue thermal history; however, they have only evaluated the cryoprobe technique [8-12].

The present paper studies cutaneous cryosurgery on a nodular BCC using LN_2 spray and emphasizes thermal history of the BCC during cryosurgical freezing. A mathematical model was established describing heat transfer within the target tissue, taking into account the anatomic structure of skin. The apparent heat capacity method was used to address the tissue phase change process. The problem was solved by FLUENT with the assumption of geometrical axisymmetry. Results of the enclosed work can be used to optimize cryospay protocol parameters which should allow improved treatment efficacy.

NOMENCLATURE

C heat capacity, J/Kg·K;
H height of BCC, mm;
h convective heat transfer coefficient, W/m^2·K;
k thermal conductivity, W/m·K;
L latent heat, J/Kg;
n normal direction of skin surface;
$\dot{q}$ heat generation rate, W/m^3;
R_0 radius of BCC, mm;
r radial coordinate, mm;
r_s radius of spray cooling area, mm;
T temperature, K;
t time, second;
V volume of tissue, m^3;
V_0 volume of BCC, m^3;
z axial coordinate, mm;

Greek

α thermal diffusivity, m^2/s;
ρ mass density, Kg/m^3;
ε mass percentage of tissue components;
ξ variable controlling thermal effect of blood perfusion;
η variable controlling thermal effect of metabolism;
τ dimensionless time;
$\dot{\omega}$ blood perfusion rate, sec.$^{-1}$;

Subscript

a air;
b blood;
epi epidermis;
f frozen;
le lethal;
LN2 liquid nitrogen;
m metabolic;
s spray;
suf skin surface;

MATHEMATICAL MODEL

Once the cryospray gun is triggered, LN_2 can be delivered directly onto the surface of the target tumor, as schematically shown in Fig. 1. A cone shield (not shown in Fig. 1) can be used to protect surrounding healthy tissue by limiting LN_2 spray to the area of the tumor with a determined margin. At the tumor surface, a heat sink forms due to LN_2 evaporation. As a result, target tumor tissue experiences a quick cooling process, followed by tissue freezing. It is well accepted that cryosurgical freezing of human tissue occurs not at a single temperature, but rather over a tissue-dependent temperature range [8, 13], implying that a phase change zone (i.e. mushy zone) exists between unfrozen and fully frozen tissues.

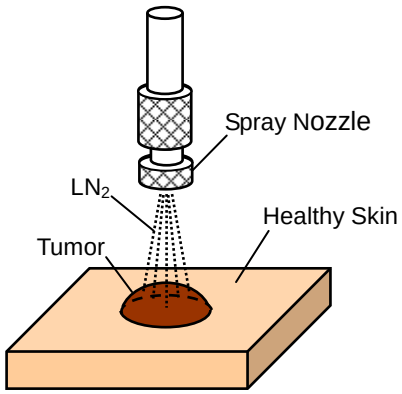

Fig. 1. Schematic of the cutaneous cryosurgery using LN_2 spray.

Human skin tissue is composed of three main layers, epidermis, dermis and subcutaneous fat, each with distinct components and physiological functions. Epidermis is the superficial, thin, avascular layer. Dermis, lying underneath epidermis, hosts abundant cutaneous capillaries, nerves and lymphatic vessels. Below dermis lies the subcutaneous fat layer, dominated by fat cells and traversed by arterial/venous pairs bifurcating from muscular vessels toward cutaneous capillaries.

Taking into account the anatomic structure described above, the present study aims to address the thermal history of skin tumor during LN_2 spray cooling. To make this quantification feasible, a series of assumptions have been implemented.

1. The studied BCC is assumed to have the geometry of a spherical cap, and the LN_2 cooling site covers a concentric circular area over the spherical cap.
2. At cooling site, sprayed cryogen and tissue have complex heat interaction, which may present the radial variation [14]. However, the quantitative information for LN_2 is to date not available. The present study therefore assumes the spray cooling is uniform over the cooling site and can be described by a convective thermal interaction with LN_2.
3. Thermal/physical properties are assumed to be homogeneous for each of the skin layers [15].
4. Thermal effects of blood perfusion and metabolism are considered in the dermis but neglected for the avascular epidermis [15].
5. In subcutaneous fat, blood perfusion effects are considered, while metabolism is ignored because the metabolism of fat occurs only in the situations of fasting, starvation and exercise [16].
6. BCC tissue is assumed to share identical thermal, physical and physiological properties with dermal tissue.
7. The freezing process of skin tissue occurs over the temperature range of $-0.5 \sim -10\ ^{o}C$ [8, 12].
8. Blood perfusion and cell metabolism cease once tissue freezing occurs [17].

The classical Pennes bioheat equation has been widely applied in the thermal modeling of biological tissue with dense capillary vasculature [10, 18]. Based on the above assumptions, Pennes equation can be utilized to describe cryosurgical heat transfer in dermal and sub-cutaneous fat tissue, as follows:

$$\rho C \frac{\partial T}{\partial t} = \nabla\left(k \cdot \nabla T\right) + \zeta \dot{\omega}_b \rho_b C_b \left(T_b - T\right) + \eta \dot{q}_m \qquad (1)$$

where the subscripts b and m represent blood and metabolism; ρ_b, C_b, and T_b respectively represent mass density (1060 Kg/m^3), specific heat (3840 J/Kg·K) and temperature (310 K) of blood [19]; $\dot{q}_m$ stands for the metabolic heat generation rate. Variables ξ and η serve to control the thermal effects of blood perfusion and metabolism heat generation during the tissue freezing process. The values of ξ and η are selected to take into account the layered structure of skin, as shown in Table 1.

Table 1. Values of variables ξ and η for three layers during the tissue freezing process.

Region	Epidermis	Dermis	Fat
Unfrozen ($T > -0.5^{o}C$)	ξ=0; η=0;	ξ=1; η=1;	ξ=1; η=0;
Mushy ($-10<T\leq-0.5\ ^{o}C$)	ξ=0; η=0;	ξ=0; η=0;	ξ=0; η=0;
Frozen ($T\leq-10\ ^{o}C$)	ξ=0; η=0;	ξ=0; η=0;	ξ=0; η=0;

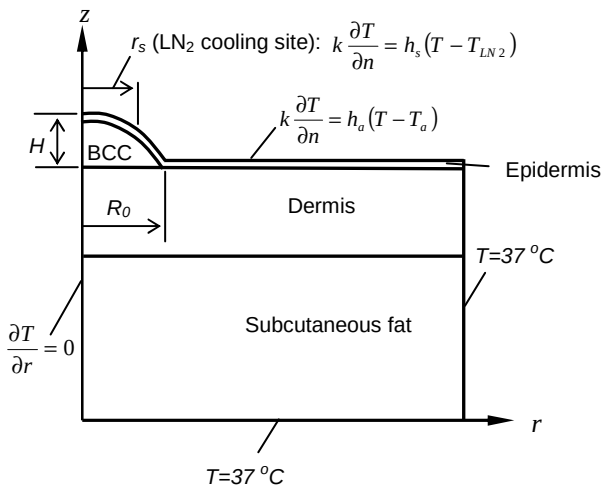

Fig. 2. Illustration of computational domain and boundary conditions.

The computational domain is established in an axisymmetric 2D space as schematically shown in Fig. 2, where the epidermis, dermis and subcutaneous fat are 0.075 mm, 1.5 mm and 3.425 mm thick, respectively [15]. The radius of the BCC, R_0, is determined to be 5 mm, and the height, H, is 2 mm. The whole domain is initially at the normal human body temperature, 37 °C. Once the spray starts, the cooling site is subject to a convective thermal boundary with a uniform heat transfer coefficient, h_s; while skin surface uncovered by LN_2 spray experiences convection heat interaction with room air, represented by a lower heat transfer coefficient, h_a:

$$k_{epi}\left.\frac{\partial T}{\partial n}\right|_{suf} = \begin{cases} h_s\left[T(r,z,t)\big|_{suf} - T_{LN2}\right] & 0 \le r \le R_0;\ 0 < t \le t_s \\ h_a\left[T(r,z,t)\big|_{suf} - T_a\right] & r > R_0;\quad 0 < t \le t_s \end{cases} \qquad (2)$$

where n represents the normal direction of the surface; t_s is the duration of the spray, selected to be 30 seconds, a commonly utilized spray duration for treatment of BCC [20]; T_{LN2} and T_a represent the LN_2 temperature, -196 °C, and the room temperature, 25 °C, respectively. The central axis is subject to the axisymmetric boundary condition. The constant temperature, 37 °C, is applied for the boundary underneath the subcutaneous fat and the one distant and parallel to the central axis, assuming spray cooling does not produce thermal perturbation on the boundaries.

The above mathematical problem was solved by a commercial software package, FLUENT (Fluent Co., New Hampshire), relying on the finite volume technique. The apparent heat capacity method was used to account for latent heat release during tissue freezing process, where the apparent heat capacity is assumed to be a linear function of temperature within the mushy zone. Grid-independent solutions can be obtained from a structured non-uniform grid with quick convergence. The grid distributes finely in BCC and the central parts of the epidermis and dermis layers, in order to observe detailed information from areas of prime concern and make computation efficient. All results reported in this paper are obtained from the grid.

THERMAL PROPERTIES IN THE STUDY

It has been noted that predicted thermal history of target tissue is greatly affected by temperature-dependent thermal properties [11]. The present study utilizes thermal and physical properties of unfrozen tissues obtained from Bowman et al. [21] and Duck [19]. Thermal conductivity and heat capacity of frozen dermal tissue are estimated based on the principle proposed by Duck [19]:

$$Y = \sum_{i=1}^{3} Y_i \varepsilon_i \qquad (3)$$

where Y represents thermal conductivity or heat capacity; the index, i , represents water, protein and lipid, which account for approximately 99% of skin tissue mass [19] and ε is the mass percentage of each component. A further assumption was made that only the properties of water are temperature-dependent referring to Alexiades and Solomon [22]. Table 2 lists the thermal and physical properties used in the study. Note the heat capacity of frozen subcutaneous fat is borrowed from data on pork fat at low temperatures [19].

Table 2. Thermal physical properties used in the study (from [19] if not otherwise indicated).

Properties	Epidermis	Dermis	Fat
k_u (W/m·K)	0.209 [(a)]	0.498	0.268
k_f (W/m·K)	0.209	$(273\text{-}T)^{1.156}$ ×0.0039+1.553 [(b)]	0.268
C_u (J/Kg·K)	3530	3150	2400
C_f (J/Kg·K)	3530	521.4 + 4.65T	piece-wise liner function
ρ (Kg/m^3)	1150	1116	916
L (J/Kg)	0	217100	70808
$\dot{q}_m$ (W/m^3)	0	1240 [(c)]	0
$\dot{\omega}_b$ (1/s)	0	0.002387 [(c)]	0.002387 [(c)]

[(a)] from [18]; [(b)] calculated from [22]; [(c)] calculated from [20].

RESULTS AND DISCUSSIONS

The success of cryosurgery relies greatly on comprehensive and in-depth understanding of cryosurgical tissue injury mechanisms. Review of the literature reveals two primary injury mechanisms: direct cell injury and vascular injury [24, 25], which are closely related to treatment tissue thermal history. It is well accepted that four parameters of thermal history are critical: lethal temperature, cooling rate (CR), hold time and thawing rate [25, 26]. The present work focuses on the study of lethal temperature and cooling rate during the cryosurgical treatment of BCC.

Lethal temperature is a highly tissue-dependent value, at which tissue can be completely destroyed. With a single free-thaw cycle, diverse lethal temperatures have been reported, ranging from -2 ~ -70 °C, for different animal tissues [24]. For skin tumors, -50 °C has been widely accepted as the lethal temperature [24, 26]. Successful treatment of BCC by cryosurgical freezing therefore requires achievement of the lethal temperature for all tumor cells.

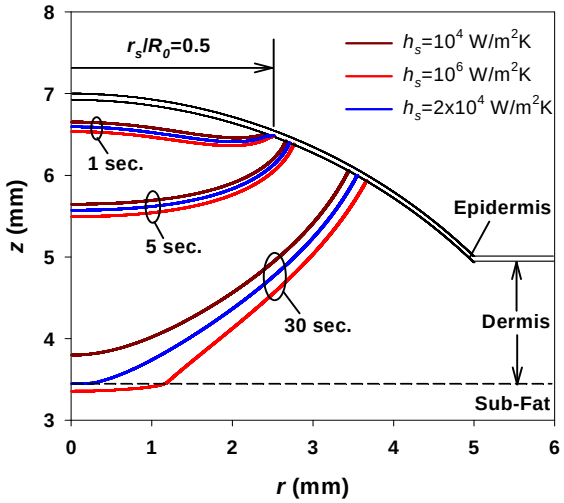

Fig. 3. The propagation of the lethal isotherm, -50 °C, when the spray cooling site covers one quarter of the protruding pathologic area of the BCC (r_s/R_0=0.5).

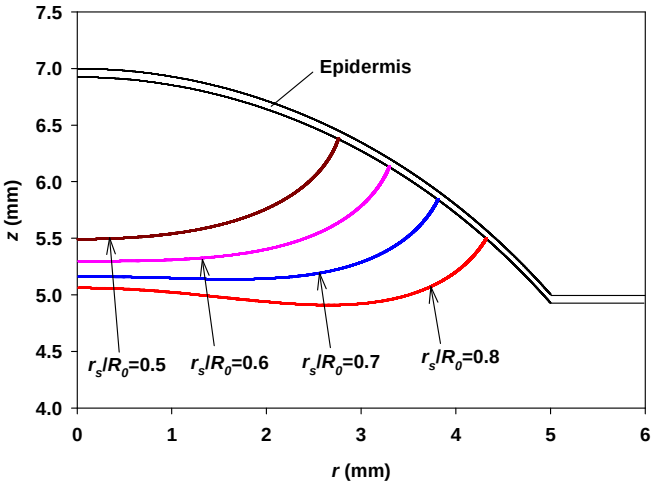

Fig. 4. Effect of cooling site area on the distribution of the lethal isotherm (t = 5 sec., h_s=10^6 W/m^2·K).

Figure 3 shows the propagation of the isotherms of the lethal temperature when radius of spray-cooling site, r_s, equals half of R_0, radius of BCC. As one can see, once spray cooling initiates, the lethal isotherm immediately forms underneath the cooling site, followed by propagation in the central and lateral directions. Comparison of lethal isotherms at 1 and 30 seconds reveals that the lethal isotherm penetrates much faster along the central as compared to the lateral axis, resulting in transformation of the lethal isotherm from the initial convex curve to a concave one.

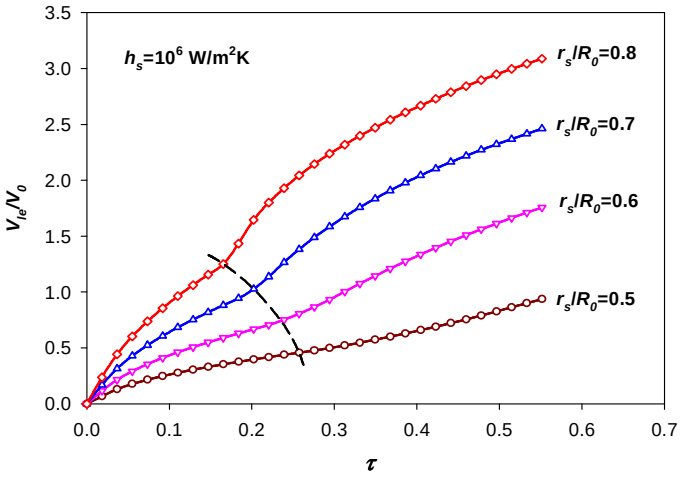

Fig. 5. Volumetric growth of tissue enclosed by lethal isotherms under different cooling site areas (h_s=10^6 W/m^2·K).

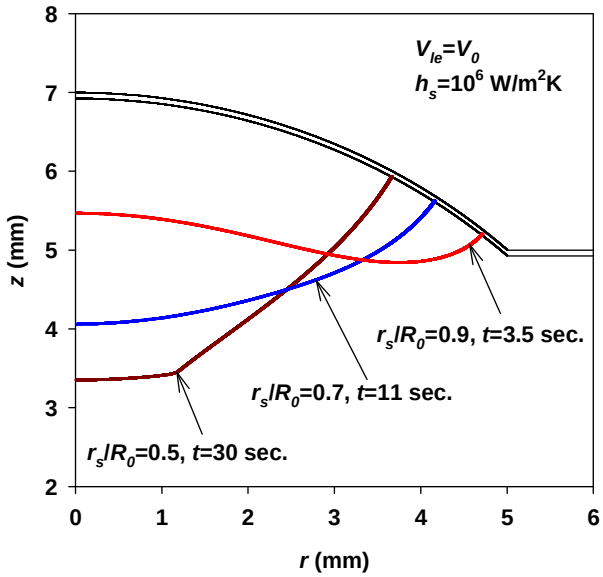

Fig. 6. Lethal isotherms enclosing the identical tissue volume as the BCC (h_s=10^6 W/m^2·K).

A parametric study was conducted for the convective heat transfer coefficient, h_s, from 10^4 to 10^6 W/m^2·K. Results indicate that propagation of the lethal isotherm is sensitive to h_s, ranging from 10^4 to 5×10^4 W/m^2·K, and little difference can be observed when h_s increases from 5×10^4 to 10^6 W/m^2·K. At 30 seconds, the lethal isotherm (h_s=10^6 W/m^2·K) penetrates through the BCC and dermal layer into the subcutaneous fat, presenting an evident inflection point at the boundary of the dermal and fatty layers, which can be understood by recalling that the two layers have distinct thermal and physical properties, as shown in Table 2.

In clinical practice, the fractional cooling technique has been developed and applied for treatment of large BCCs (≥ 10mm in diameter) in order to minimize scarring and achieve the best cosmetic outcome. In this technique, the cooling site of the first freezing process only covers a partial surface area of the BCC [24]. Thus, the effect of cooling site area on the lethal isotherm distribution also deserves study. Figure 4 shows the distribution of lethal isotherms with varied cooling site radii, while other parameters are identical: t = 5 seconds, h_s=10^6 W/m^2·K. It can be seen that at 5 seconds, the lethal isotherm for r_s/R_0=0.5 has already progressed to a concave curve, while at r_s/R_0=0.8 convex geometry is still present. One can also see that increased cooling site area results in accelerated propagation of the lethal isotherm along the central axis. Rotation of the isotherms around the central axis will produce curved isotherm surfaces, which, within the epidermis, enclose different volumes of tissue. The comparison of volumes under different cooling site areas is shown in Fig. 5.

Figure 5 uses the dimensionless parameter, V_{le}/V_0, to represent tissue volume, where V_{le} is the volume enclosed by the lethal isotherm surface and V_0 is the volume of BCC, i.e. the protruding spherical cap in Fig. 2. Dimensionless time, τ, is defined as follows:

$$\tau = \frac{\bar{\alpha} \cdot t}{R_0^2} \tag{4}$$

where R_0 is the radius of the BCC (5 mm) and $\bar{\alpha}$ is the temperature averaged thermal diffusivity of dermal tissue, which can be calculated according to:

$$\bar{\alpha} = \frac{\bar{k}}{\rho \bar{C}} \tag{5}$$

In Equation (5), $\bar{k}$ and $\bar{C}$ are temperature averaged thermal conductivity and heat capacity, which can be obtained by:

$$\bar{k} = \frac{\int_{223}^{310} k(t)dt}{310-223} \tag{6}$$

and

$$\bar{C} = \frac{\int_{223}^{310} C(t)dt}{310-223} \tag{7}$$

The temperature dependent functions, $k(t)$ and $C(t)$ are defined in Table 2.

In Fig. 5, it is evident that there exists an inflection point on each curve (connected by the dash line in the figure). Careful study of the temperature field reveals that inflection of the curve occurs when the frozen zone propagates into the subcutaneous fat. In other words, the dash line in the figure outlines the r_s dependent threshold value of the freezing time, which marks the instant when the ice ball extends into the subcutaneous fat. From Fig. 5 one can also see that increasing the cooling site can significantly enhance the efficiency of the cooling process. At any instant, the tissue volume enclosed by the lethal isotherm surface with r_s=0.6R_0 almost doubles that of r_s=0.5R_0. The same value may be even tripled using r_s=0.8R_0. Therefore, in order to achieve lethal temperature for a certain volume of tissue, a spray with a smaller cooling site requires more time.

Figure 6 shows three lethal isotherms, which enclose tissue volume identical with our proposed BCC, i.e. V_{le}/V_0 equals 1.0, with the heat transfer coefficient, h_s, equal to10^6 W/m^2·K. In order to achieve V_{le}/V_0=1.0, the spray of r_s/R_0=0.9 needs 3.5

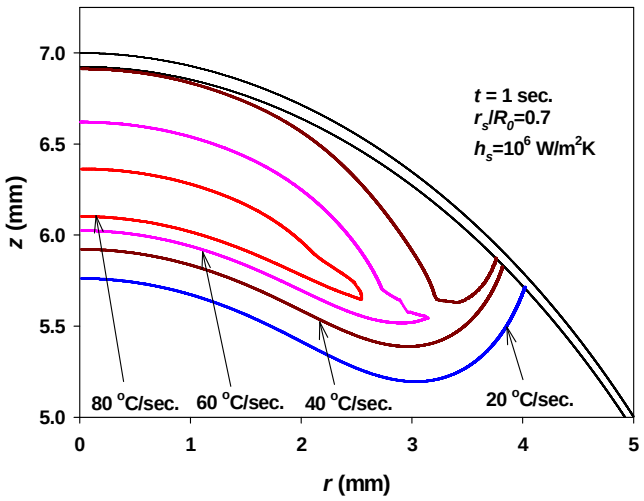

Fig. 7. Contours of the CR in the BCC: r_s/R_0=0.7, h_s=10^6 W/m^2·K, t=1 sec.

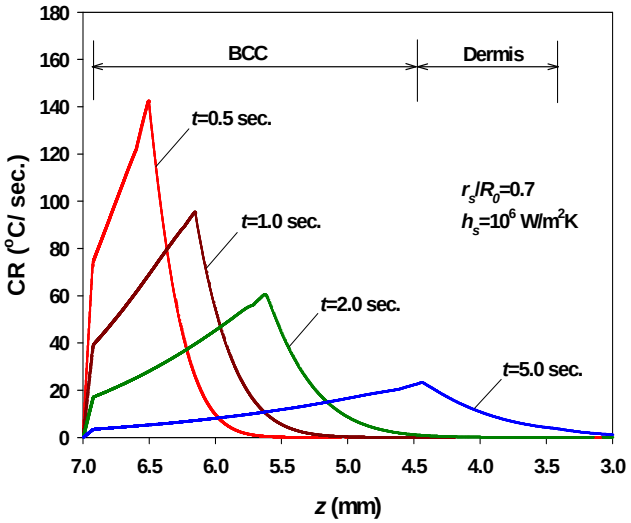

Fig. 8. Variation of CR along the central axis when r_s/R_0=0.7 and h_s=10^6 W/m^2·K.

seconds while that of r_s/R_0=0.5 requires 30 seconds. The three isotherms have distinct geometries: the one with r_s/R_0=0.9 is convex, flat and wide, compared with the one with r_s/R_0=0.5, which has a relatively narrow lateral span and deep penetration along the central axis. Ideally, freezing should completely destroy malignant tissue while sparing healthy tissue. For the BCC currently under study, a spray with r_s=0.9R_0 has reasonable cooling efficiency but will incorporate greater non-tumor tissue generating a larger final scar. In practice, Figures 3 – 6 can be used to determine spray with optimal cooling site area and cooling time to achieve tumor destruction with minimal injury to non-involved tissue.

Another critical parameter of cryosurgical tissue thermal history is cooling rate (CR), the primary determinant for tissue injury. Studies of cryosurgical tissue injury indicate that target tissue can be destroyed primarily by two mechanisms: solution-effect and intracellular ice formation (IIF) [24, 25]. Solution-effect happens when tissue freezes with a slow CR, while a sufficiently high CR can lead to IIF. During tissue freezing, ice formation occurs extracellularly first, leading to increased concentration of the extracellular solution. Then, due to the concentration difference, intracellular water transports through the cell membrane. Slow cooling provides enough time for mass transfer of intracellular water, resulting in cell dehydration and concentration of intracellular electrolytes, the so-called solution-effect. Solution-effect injures the cell in several ways, e.g. damage to the enzymatic machinery and cell membrane destabilization [25]. On the other hand, if tissue freezes with a sufficiently high CR, there is inadequate time for water transport and IIF results. IIF is lethal to living cells because intracellular ice crystals disrupt cell membranes and intracellular organelles [24].

Figure 7 shows the contours of CR under the conditions of r_s/R_0=0.7, h_s=10^6 W/m^2·K and t=1 sec. Each point on the contour has the identical CR, as indicated in the figure. It can be seen that at 1 second, tissue with high CR (e.g. CR ≥ 20 °C/sec.) is close to the spray cooling site, while the majority of the tissue (below the blue curve in the figure) experiences a relatively low CR. Examination of CR contours at consecutive moments reveals that the CR presents a highly dynamic distribution during the cooling process, which can be explored in detail by studying the variation of the CR along the central axis (Fig. 8).

The abscissa of Fig. 8, from left to right, represents the central axis (z axis in Fig. 2) going through the epidermis, BCC, dermis and subcutaneous fat. As one can see, each CR distribution curve presents a maximum value, which decreases quickly from 140 °C/s (t=0.5 sec.) to 20 °C/s (t=5 sec.). The position of the peak value also changes with time. For example, at t=1 sec., the highest CR occurs at z≈6.15 mm, while 4 seconds later, the position of the peak value moves to z≈4.44 mm. Since a high CR is necessary for IIF, Fig. 8 implies that IIF will happen in tissue close to the skin surface and the IIF zone will grow only at the early stage of the cooling process. In later stages, tissue will be subject to a low CR, precluding IIF. The temporal distributions of CR and temperature can be used to determine the IIF zone, but will not be discussed here due to space limitations.

CONCLUSIONS

A mathematical model, using Pennes equation to describe heat transfer within tissue, is provided for cutaneous cryosurgery of a nodular BCC using LN_2 spray. The computation domain composes epidermis, BCC, dermis and subcutaneous fat, accommodating the effects of geometry and anatomic tissue structure. Thermal interaction between LN_2 and underlying tissue is simplified by a convective thermal boundary, represented by a constant heat transfer coefficient. Analysis concentrates on variation of lethal isotherms and CR in target issue, and a parametric study has been presented on the heat transfer coefficient, h_s, the cooling site area and the spray time. Calculation results indicate that the lethal isotherm penetrates much faster along the central as compared to the lateral axis. Lethal isotherm propagation is sensitive to h_s in the

range of 10^4~5×10^4 W/m^2·K. Further, volume enclosed by the lethal isotherm is increased by increasing the cooling site area, resulting in improved cooling efficiency. Tissue CR is dynamic during the cryospray procedure, maximum CR decreases quickly as treatment proceeds, and the high CR zone moves from near the skin surface to deeper tissue. This model can be used as a tool for LN_2 spray cryosurgery planning. Effect of alternative protocol parameters, e.g. cooling site area and spray time, can be evaluated and values can be chosen to achieve optimal outcome.

REFERENCES

1. Agnieszka, K. and Noah S., Evidence-based review of the use of cryosurgery in treatment of basal cell carcinoma, *Dermatol. Surg.*, 2003. **29**(6): p. 566-571.
2. Hodgson, S.V. and Maher E. R., *A Practical Guide to Human Cancer Genetics*. 1993: Cambridge University Press. p. 99-100.
3. Kuijers, D.I.M., Thissen M.R.T.M., and Neumann M.H.A., Basal cell carcinoma: treatment options and prognosis, a scientific approach to a common malignancy, *Am. J. Clin. Dermatol*, 2002. **3**(4): p. 247-259.
4. Freedberg, I.M., *Fitzpatrick's Dermatology in General Medicine (5th ed.)*. 1999, New York: McGraw-Hill, Health Professions Division: p. 857.
5. White, C.A., Liquid Air: Its Application in Medicine and Surgery, *Med. Rec.*, 1899. **56**: p. 109-112.
6. Chang, Z.H., et al., Development of a High-Performance Multiprobe Cryosurgical Device, *Medical Instrumentation & Technology*, 1994: p. 383-390.
7. Kuflik, E.G. and Gage A.A., *Cryosurgical Treatment for Skin Cancer*, 1990: IGAKU-SHOIN Medical Publishers, Inc.
8. Comini, G. and Giudice S.D., Thermal aspects of cryosurgery, *Journal of Heat Transfer*, 1976: p. 543-549.
9. Weill, A., Shitzer A., and Bar-Yoseph P., Finite element analysis of the temperature field around two adjacent cryo-probes, *Journal of Biomechanical Engineering*, 1993. **115**: p. 374-379.
10. Rabin, Y. and Shitzer A., Numerical solution of the multidimensional freezing problem during cryosurgery, *Journal of Biomechanical Engineering*, 1998. **120**: p. 32-37.
11. Smith, D.J., Devireddy R.V., and Bischof J.C., Prediction of thermal history and interface propagation during freezing in biological systems - latent heat and temperature-dependent property effects, *5th ASME/JSME Joint Thermal Engineering Conference*. 1999. San Diego, California.
12. Hoffmann, N.E. and Bischof J.C., Cryosurgery of normal and tumor tissue in the dorsal skin flap chamber: part I-thermal response, *Journal of Biomechanical Engineering, 2001*. **123**: p. 301-309.
13. Rabin, Y. and Shitzer A., Exact solution to the one-dimensional inverse-Stefan problem in nonideal biological tissues, *Journal of Heat Transfer*, 1995. **117**: p. 425-431.
14. Franco, W., et al., Radial and temporal variations in surface heat transfer during cryogen spray cooling, *Physics in Medicine and Biology*, 2005. **50**: p. 387-397.
15. Diller, K.R. and Hayes L.J., A finite element model of burn injury in blood-perfused skin, *Journal of Biomechanical Engineering*, 1983. **105**: p. 300-307.
16. Philip A Wood, *How Fat Works*, Harvard University Press, 2006, p.84-85.
17. Zhang, J., et al., Numerical simulation for heat transfer in prostate cancer cryosurgery, *Journal of Biomechanical Engineering*, 2005. **127**: p. 279-294.
18. Charny, C.K., Mathematical Models of Bioheat Transfer, *Advances in Heat Transfer*, Vol. 22. 1992.
19. Duck, F.A., *Physical properties of Tissue*. 1990, San Diego, CA: Academic Press Limited.
20. Mallon, E. and Dawber R., Cryosurgery in the treatment of basal cell carcinoma, *Dermatol. Surg.*, 1996, **22**: p. 854-858.
21. Bowman, H.F., Cravaho E.G., and Woods M., Theory, measurement, and application of thermal properties of biometerials, *Ann. Rev. Biophys. Bioeng.*, 1975, **4**: p. 43-80.
22. Alexiades, A. and Solomon A.D., *Mathematical Modeling of Melting and Freezing Processes*. 1993, Washington D.C.: Hemisphere.
23. Shitzer, A. and Eberhart R.C., *Heat Transfer in Medicine and Biology: Analysis and Applications (I)*. Vol. 1. 1985: Plenum Press.
24. Gage, A.A. and Baust J., Mechanisms of Tissue Injury in Cryosurgery, *Cryobiology*, 1998. **37**: p. 171-186.
25. Hoffmann, N.E. and Bischof J.C., The cryobiology of cryosurgical injury, *Urology*, 2002. **60 (Supplement 2A)**: p. 40-49.
26. Gage, A.A., et al., Sensitivity of pigmented mucosa and skin to freezing injury, *Cryobiology*, 1979. **16**: p. 348-361.